Immunoprecipitation and two-hybrid assays

Transfected cells were washed with PBS and treated with RIPA buffer with no SDS. Mouse monoclonal antibody against Flag (M2, Sigma) was added to cell extract and incubated overnight at 4 °C. Protein-A-conjugated Sepharose equilibrated in RIPA was then added and incubated for 2 h. The beads were extensively washed with ice-cold RIPA and the precipitate was dissolved in a sample buffer. Polyclonal antibody against p65 (Rockland) was used for western blot analysis. For mammalian two-hybrid experiments, the *ING4* gene was subcloned in-frame into pBIND and fused with the yeast GAL4 DNA-binding domain. p65 was subcloned in-frame into pACT and fused to the VP16 activation domain of herpes simplex virus. A series of constructs was used as controls: pBIND–Id and pACT–MyoD, containing GAL4–Id and VP16–MyoD fusion proteins, respectively, were used as positive controls; and pBIND and pACT, pBIND–ING4 and pACT, and pBIND and pACT–p65 were used as negative controls. Protein–protein interaction was determined by the activation of firefly luciferase.

Reporter gene assay

Cells (1×10^5 per well) were transfected with plasmids containing NF-κB-binding elements by Lipofectamine (Invitrogen). Two days after transfection, cells were lysed in Reporter Lysis Buffer (Promega), and luciferase activity was measured by a luminometer using an Enhanced Luciferase Assay kit (BD Biosciences).

Electrophoretic mobility shift assay

We carried out electrophoretic mobility shift assays (EMSAs) on nuclear extracts prepared as described[25] using the following double-stranded oligonucleotides: NF-κB, 5′-AGT TGA GGG GAC TTT CCC AGG C-3′; and nonspecific oligonucleotide (Oct-1), 5′-TGT CGA ATG CAA ATC ACT AGA A-3′. The oligonucleotide was 5′-end-labelled with biotin and annealed by standard procedures. Binding reaction was carried out by pre-incubating nuclear extract protein (5 μg) in 2.5% glycerol, 1 μg of poly(dI-dC), 50 mM KCl and 5 mM $MgCl_2$ at room temperature for 15 min. For competition assays, we added a tenfold molar excess of unlabelled oligonucleotide to the binding reaction. Samples were loaded on a 5% polyacrylamide gel. Electrophoresis was done at room temperature for 3 h at 100 V. The gel was then transferred to a nylon membrane and the biotin end-labelled DNA was detected using streptavidin-conjugated horseradish peroxidase. For supershift assay, antibody against p65 (Santa Cruz Biotech) was added to the binding reaction for 45 min on ice.

Received 16 October 2003; accepted 9 January 2004; doi:10.1038/nature02329.

1. Maher, E. A. *et al.* Malignant glioma: genetics and biology of a grave matter. *Genes Dev.* **15,** 1311–1333 (2001).
2. Plate, K. H. & Risau, W. Angiogenesis in malignant gliomas. *Glia* **15,** 339–347 (1995).
3. Kerbel, R. & Folkman, J. Clinical translation of angiogenesis inhibitors. *Nature Rev. Cancer* **2,** 727–739 (2002).
4. Carmeliet, P. & Jain, R. K. Angiogenesis in cancer and other diseases. *Nature* **407,** 249–257 (2000).
5. Van Meir, E. G. *et al.* Release of an inhibitor of angiogenesis upon induction of wild type p53 expression in glioblastoma cells. *Nature Genet.* **8,** 171–176 (1994).
6. Dameron, K. M., Volpert, O. V., Tainsky, M. A. & Bouck, N. Control of angiogenesis in fibroblasts by p53 regulation of thrombospondin-1. *Science* **265,** 1582–1584 (1994).
7. Garkavtsev, I., Kazarov, A., Gudkov, A. & Riabowol, K. Suppression of the novel growth inhibitor $p33^{ING1}$ promotes neoplastic transformation. *Nature Genet.* **14,** 415–420 (1996).
8. Garkavtsev, I. & Riabowol, K. Extension of the replicative lifespan of human diploid fibroblasts by inhibition of the $p33^{ING1}$ candidate tumour suppressor. *Mol. Cell. Biol.* **17,** 2014–2019 (1997).
9. Garkavtsev, I. *et al.* The candidate tumour suppressor $p33^{ING1}$ cooperates with p53 in cell growth control. *Nature* **391,** 295–298 (1998).
10. Shiseki, M. *et al.* $p29^{ING4}$ and $p28^{ING5}$ bind to p53 and p300, and enhance p53 activity. *Cancer Res.* **63,** 2373–2378 (2003).
11. Skowyra, D. *et al.* Differential association of products of alternative transcripts of the candidate tumour suppressor ING1 with the mSin3/HDAC1 transcriptional corepressor complex. *J. Biol. Chem.* **276,** 8734–8739 (2001).
12. Nourani, A. *et al.* Role of an ING1 growth regulator in transcriptional activation and targeted histone acetylation by the NuA4 complex. *Mol. Cell. Biol.* **21,** 7629–7640 (2001).
13. Leung, K. M. *et al.* The candidate tumour suppressor ING1b can stabilize p53 by disrupting the regulation of p53 by MDM2. *Cancer Res.* **62,** 4890–4893 (2002).
14. Toyama, T. *et al.* Suppression of ING1 expression in sporadic breast cancer. *Oncogene* **18,** 5187–5193 (1999).
15. Oki, E., Maehara, Y., Tokunaga, E., Kakeji, Y. & Sugimachi, K. Reduced expression of $p33^{ING1}$ and the relationship with p53 expression in human gastric cancer. *Cancer Lett.* **147,** 157–162 (1999).
16. Chen, B., Campos, E. I., Crawford, R., Martinka, M. & Li, G. Analyses of the tumour suppressor ING1 expression and gene mutation in human basal cell carcinoma. *Int. J. Oncol.* **22,** 927–931 (2003).
17. Gunduz, M. *et al.* Genomic structure of the human ING1 gene and tumour-specific mutations detected in head and neck squamous cell carcinomas. *Cancer Res.* **60,** 3143–3146 (2000).
18. Brat, D. J., Castellano-Sanchez, A., Kaur, B. & Van Meir, E. G. Genetic and biologic progression in astrocytomas and their relation to angiogenic dysregulation. *Adv. Anat. Pathol.* **9,** 24–36 (2002).
19. Kleihues, P. *et al.* The WHO classification of tumours of the nervous system. *J. Neuropathol. Exp. Neurol.* **61,** 215–225 (2002).
20. Jain, R. K., Munn, L. L. & Fukumura, D. Dissecting tumour pathophysiology using intravital microscopy. *Nature Rev. Cancer* **2,** 266–276 (2002).
21. Ghosh, S. & Karin, M. Missing pieces in the NF-κB puzzle. *Cell* **109** (suppl.), S81–S96 (2002).
22. Karin, M., Cao, Y., Greten, F. R. & Li, Z. W. NF-κB in cancer: from innocent bystander to major culprit. *Nature Rev. Cancer* **2,** 301–310 (2002).
23. Desbaillets, I., Diserens, A. C., de Tribolet, N., Hamou, M. F. & Van Meir, E. G. Regulation of interleukin-8 expression by reduced oxygen pressure in human glioblastoma. *Oncogene* **18,** 1447–1456 (1999).
24. Desbaillets, I., Diserens, A. C., Tribolet, N., Hamou, M. F. & Van Meir, E. G. Upregulation of interleukin 8 by oxygen-deprived cells in glioblastoma suggests a role in leukocyte activation, chemotaxis, and angiogenesis. *J. Exp. Med.* **186,** 1201–1212 (1997).
25. Xu, L., Xie, K., Mukaida, N., Matsushima, K. & Fidler, I. J. Hypoxia-induced elevation in interleukin-8 expression by human ovarian carcinoma cells. *Cancer Res.* **59,** 5822–5829 (1999).

Supplementary Information accompanies the paper on **www.nature.com/nature.**

Acknowledgements We thank E. di Tomaso, P. Vitello, S. Roberge and A. Merkulova for technical assistance; and B. Seed, D. Fukamura and D. Duda for comments on the manuscript. This work was supported by grants from the National Cancer Institute.

Competing interests statement The authors declare that they have no competing financial interests.

Correspondence and requests for materials should be addressed to I.G. (igorg@steele.mgh.harvard.edu).

Survival signalling by Akt and eIF4E in oncogenesis and cancer therapy

Hans-Guido Wendel[1], Elisa de Stanchina[1], Jordan S. Fridman[1]*, Abba Malina[2], Sagarika Ray[1], Scott Kogan[3], Carlos Cordon-Cardo[4], Jerry Pelletier[2] & Scott W. Lowe[1]

[1]*Cold Spring Harbor Laboratory, Cold Spring Harbor, New York 11724, USA*
[2]*McGill University, Montreal, H3G1Y6, Quebec, Canada*
[3]*University of California-San Francisco, San Francisco, California 94143-0128, USA*
[4]*Department of Pathology, Memorial Sloan-Kettering Cancer Center, New York, New York 10021, USA*

* Present address: Incyte Corporation, Wilmington, Delaware 19880, USA

Evading apoptosis is considered to be a hallmark of cancer, because mutations in apoptotic regulators invariably accompany tumorigenesis[1]. Many chemotherapeutic agents induce apoptosis, and so disruption of apoptosis during tumour evolution can promote drug resistance[2]. For example, Akt is an apoptotic regulator that is activated in many cancers and may promote drug resistance *in vitro*[3]. Nevertheless, how Akt disables apoptosis and its contribution to clinical drug resistance are unclear. Using a murine lymphoma model, we show that Akt promotes tumorigenesis and drug resistance by disrupting apoptosis, and that disruption of Akt signalling using the mTOR inhibitor rapamycin reverses chemoresistance in lymphomas expressing Akt, but not in those with other apoptotic defects. eIF4E, a translational regulator that acts downstream of Akt and mTOR, recapitulates Akt's action in tumorigenesis and drug resistance, but is unable to confer sensitivity to rapamycin and chemotherapy. These results establish Akt signalling through mTOR and eIF4E as an important mechanism of oncogenesis and drug resistance *in vivo*, and reveal how targeting apoptotic programmes can restore drug sensitivity in a genotype-dependent manner.

Apoptosis is controlled by a complex network of proliferation and survival genes that is frequently disrupted during tumour evolution. For example, the phosphatidylinositol-3-OH kinase (PI(3)K) pathway integrates receptor tyrosine kinase signalling with the apoptotic network[4,5]. One mediator of PI(3)K signalling is the Akt/protein kinase B (PKB) kinase, which phosphorylates multiple downstream effectors that ultimately produce global changes in cellular physiology. How Akt promotes survival is controversial, but it may involve direct phosphorylation of apoptotic regulators, increased cell cycle progression, decreased transcription of pro-apoptotic genes through inhibition of forkhead transcription factors, altered metabolism, or changes in the translation of messenger RNAs that ultimately control cell death[5].

Mutations that activate the PI(3)K–Akt pathway, including amplifications of PI(3)K pathway components and inactivation of the negative regulator PTEN, are common in human malignancies[6–8]. Therefore, drugs that inhibit Akt or its downstream effectors may be effective against many human cancers.

To determine how Akt signalling influences tumorigenesis and treatment responses *in vivo*, we compared the effects of a constitutively activated Akt mutant[9] to the anti-apoptotic regulator Bcl-2 in the Eμ-*Myc* model of B-cell lymphoma[10]. Eμ-*Myc* haematopoietic stem cells (HSCs) isolated from fetal livers were transduced with Akt- or Bcl-2-expressing retroviruses and transplanted into lethally irradiated mice[11], and the chimaeric recipients were monitored for lymphoma onset and pathology (Fig. 1a). The resulting lymphomas were each transplanted into several wild-type animals, where they produced malignancies that were pathologically indistinguishable from the original disease[12]. These animals were then treated with a chemotherapeutic regime and monitored for time to relapse (tumour-free survival) and overall survival by lymph node palpation and blood analysis (Fig. 1b). This approach allows a rapid analysis of genotype–response relationships in a natural setting using methods that parallel human clinical trials.

As with Bcl-2 (ref. 12), Akt markedly accelerated lymphomagenesis relative to controls (Fig. 2a, $P < 0.0001$ for both Akt and Bcl-2 relative to murine stem cell virus (MSCV)). Compared with lymphomas arising in Eμ-*Myc* mice, the Akt and Bcl-2 lymphomas were more invasive and were often associated with leukaemia (Fig. 2d, and data not shown). Immunophenotyping revealed that Akt and Bcl-2 lymphomas were derived from a B220/CD45R-positive progenitor cell that lacked other markers of B-cell differentiation, whereas control lymphomas were typically derived from a more mature B-cell type (Fig. 2b; see also Supplementary Fig. 1 and Supplementary Table 1). Although lymphomas of all genotypes proliferated rapidly as assessed by Ki-67 staining, Akt and Bcl-2 lymphomas showed much less apoptosis relative to controls as measured by a TdT-mediated dUTP nick end labelling (TUNEL) assay (Fig. 2c). The impact of Akt on tumour behaviour was reminiscent of *p53* tumour suppressor gene loss, which accelerates Myc-induced lymphomagenesis by disabling apoptosis[11]. In fact, whereas all lymphomas arising from $p53^{+/-}$ Eμ-*Myc* HSCs lost the wild-type *p53* allele, those expressing either Bcl-2 or Akt did not (Supplementary Fig. 2). Therefore, Akt can compensate for *p53* loss during tumorigenesis and acts in a manner that is temporally and pathologically similar to a strictly anti-apoptotic gene.

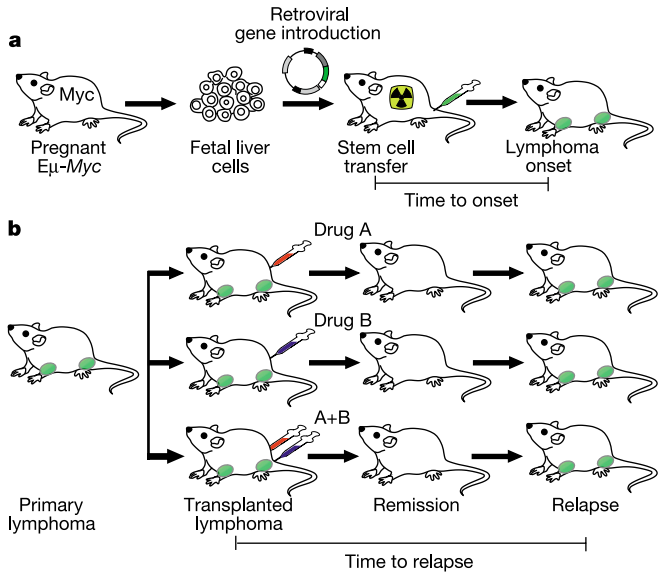

Figure 1 Integrated model of lymphomagenesis and treatment response.

Next, C57BL/6 mice harbouring different transplanted lymphomas were treated with cyclophosphamide (cytoxan, CTX) or doxorubicin (DXR) and monitored for tumour-free and overall survival (Fig. 2e, f; see also Supplementary Fig. 3). Here, animals harbouring *Arf*-null lymphomas were used as controls, as these lymphomas are also highly aggressive but remain chemosensitive[13]. After CTX therapy, mice harbouring control lymphomas invariably entered a complete remission and >50% remained tumour free after 100 days. In contrast, mice harbouring Akt lymphomas responded poorly, typically displaying remissions of less than 20 days with no long-term survivors ($P < 0.001$ relative to controls). Although DXR produced fewer long-lasting remissions in the control cohort than CTX, mice harbouring Akt lymphomas still displayed substantial reductions in tumour-free and overall survival (Fig. 2f; see also Supplementary Fig. 3b, $P < 0.0001$ for Akt and Bcl-2 versus control). Therefore, Akt-mediated survival signalling can promote drug resistance *in vivo*.

We next investigated whether pharmacologically inhibiting the pathway downstream of Akt might have anti-tumour effects. One established Akt effector is mTOR, a serine/threonine kinase implicated in translation control, which can be potently inhibited by the immunosuppressant rapamycin[14]. Although not considered to be a primary component of Akt survival signalling, mTOR can mediate metabolic changes important for cell survival in growth-factor-poor environments[15,16]. Rapamycin has had modest anti-tumour activity against PTEN-deficient tumours in animal studies, and can potentiate drug-induced cell death *in vitro*[17–20]. We therefore asked whether rapamycin was effective against our defined murine lymphomas, and whether its activity was genotype-dependent or enhanced by chemotherapy.

To determine whether rapamycin inhibits mTOR in Eμ-*Myc* lymphomas, its activity was indirectly assessed in extracts from untreated or treated lymphomas using antibodies that specifically recognize the phosphorylated forms of two mTOR targets: the ribosomal S6 protein (which is phosphorylated by the S6 kinase) and eIF4G. As expected, untreated Akt lymphomas expressed substantially more phosphorylated S6 and eIF4G relative to Bcl-2 lymphomas (Fig. 3a, compare lanes 1 and 5). Treatment with rapamycin alone or in combination with chemotherapy substantially reduced S6 and eIF4G phosphorylation in Akt lymphomas (Fig. 3a, compare lanes 1–3 and 4). Hence, rapamycin inhibits mTOR activity *in vivo* in a manner that is not affected by conventional therapies.

We then examined the acute and long-term effects of rapamycin *in vivo*. In Akt lymphomas, rapamycin treatment produced only a slight increase in apoptosis relative to untreated counterparts 6 h after therapy, as assessed by PARP cleavage in lymphoma extracts (Fig. 3a, compare lanes 1 to 3) and by TUNEL staining of lymphoma sections (Fig. 3b). Accordingly, these mice rarely achieved complete remissions (Fig. 4a, b) and they showed tumour-free and overall survival patterns that were no better than those produced by conventional therapy (Fig. 4c; see also Supplementary Fig. 4). Furthermore, rapamycin displayed even less activity against lymphomas of other genotypes (Figs 3 and 4). Therefore, despite its ability to inhibit mTOR *in vivo*, rapamycin had only modest activity as a single agent.

In marked contrast, the combination of chemotherapy and rapamycin showed potent activity against Akt-expressing lymphomas. For example, DXR and rapamycin treatment produced PARP cleavage and massive apoptosis 6 h after therapy (Fig. 3a, compare lanes 1 and 4; see also panel b), with all of the animals achieving complete remissions (Fig. 4a, b; see also Supplementary Fig. 6 for a comparison of matched groups). Indeed, the combination of DXR and rapamycin produced more complete remissions and better tumour-free survival in the otherwise drug-resistant Akt lymphomas than DXR produced in the chemosensitive controls (Fig. 4a, c, $P < 0.001$ for rapamycin plus DXR versus DXR or rapamycin

alone), resulting in a substantial survival benefit (Supplementary Fig. 4a, $P < 0.001$ for rapamycin plus DXR versus DXR or rapamycin alone). Similar effects were observed with the combination of CTX and rapamycin, where approximately half of the mice achieved remissions lasting more than 60 days compared with none for either agent alone (Supplementary Figs 4b and 5a, $P < 0.001$). Consequently, rapamycin reverses the apoptotic defects and drug resistance occurring in Akt lymphomas.

These potent effects were not observed in lymphomas of other genotypes. Bcl-2 lymphomas, which showed a similar drug-resistance profile to either rapamycin or chemotherapy alone, remained non-responsive to a combination of the two treatments as assessed in both acute and long-term assays (Fig. 4a, d; see also Supplementary Figs 4c, d and 5b). Moreover, control lymphomas, which were initially chemosensitive, showed no improvement in short- or long-term responses after combination therapy, and, in fact, rapamycin appeared to antagonize drug-induced apoptosis in these cells (Fig. 3b and our own unpublished observations). Therefore, although each lymphoma studied contained an anti-apoptotic lesion, the chemosensitizing effects of rapamycin were specific for tumours with constitutive Akt signalling.

The results described above suggest that mTOR is essential for Akt-mediated survival signalling. mTOR normally regulates translation in response to nutrients and growth factors by phosphorylating key components of the protein synthesis machinery, including the above mentioned ribosomal protein S6 kinase, $p70^{S6K}$ and the 4E-BP proteins[21]. Phosphorylation of 4E-BP, in turn, releases the translation initiation factor eIF4E to stimulate cap-dependent translation. Although its role in oncogenesis is poorly understood, eIF4E can have transforming and anti-apoptotic activities *in vitro*[22,23] and is overexpressed in some tumour types[24]. Furthermore, Akt-expressing tumours selectively increase the translation of some mRNAs in a rapamycin-reversible manner[25,26]. Therefore, to examine further the effects of translational control on tumour phenotypes, we directly compared eIF4E to Akt in the Eμ-*Myc* model (see Fig. 1).

eIF4E accelerated lymphomagenesis in a manner that was similar to Akt (Fig. 5a, median onset of 42.5 and 50 days for Akt and eIF4E, respectively; $P < 0.0001$ versus control). Moreover, as with Akt lymphomas, eIF4E lymphomas displayed a disseminated pathology and a high proliferation/apoptosis ratio (Fig. 5b), despite only an approximately 2.5-fold increase in eIF4E protein (Fig. 5c, compare lanes 1 to 3; see also Supplementary Fig. 7). eIF4E could also compensate for *p53* loss during lymphomagenesis, as lymphomas arising from $p53^{+/-}$ Eμ-*Myc* HSCs retained the wild-type *p53* allele (Supplementary Fig. 2). Despite these similarities, eIF4E

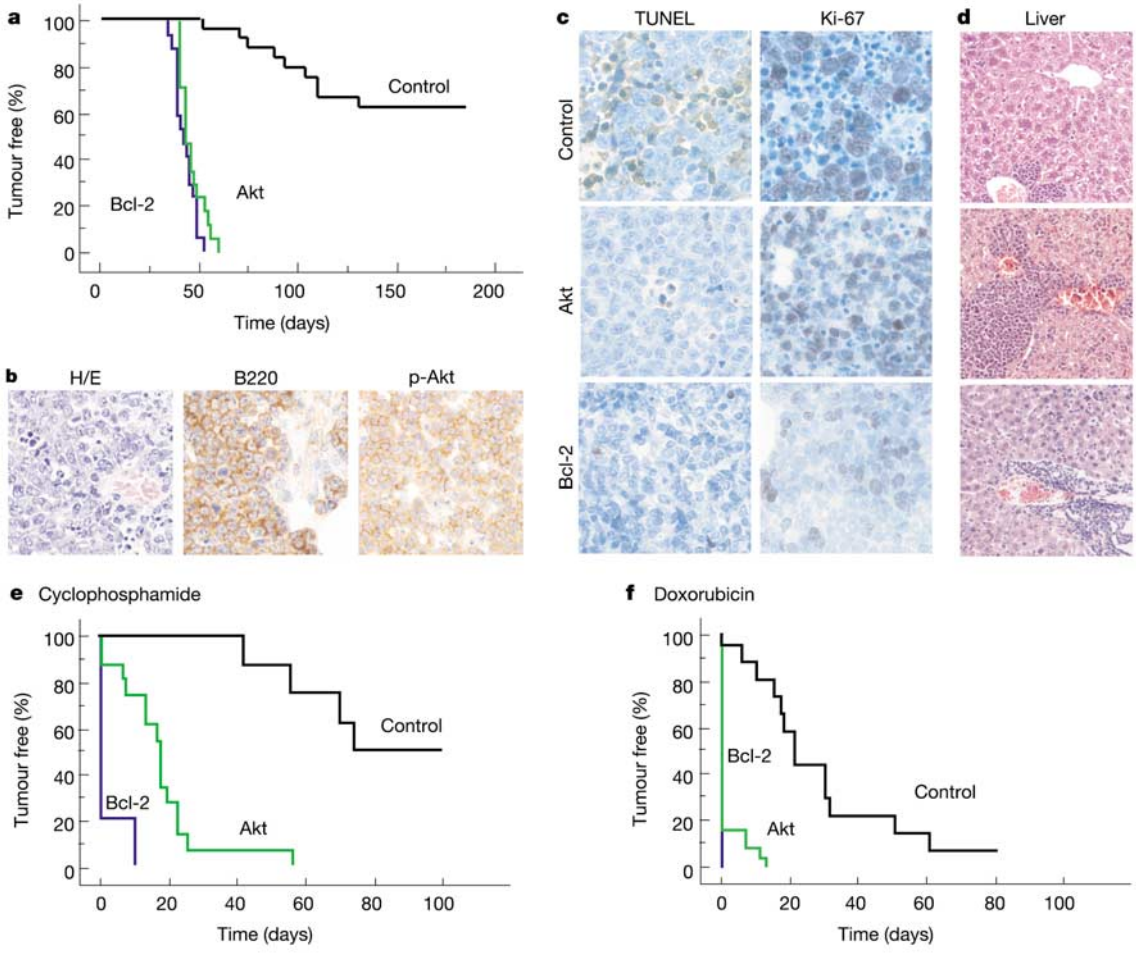

Figure 2 Akt accelerates lymphomagenesis and promotes drug resistance *in vivo*. **a**, Kaplan–Meier plot showing tumour onset in mice reconstituted with Eμ-*Myc* HSCs transduced with MSCV ($n = 40$, black), Akt ($n = 18$, green) or Bcl-2 ($n = 18$, blue). A kinase-dead mutant Akt (K179A) did not accelerate lymphomagenesis, and Akt did not cause tumour formation in non-transgenic HSCs (data not shown). **b**, Representative micrographs of Eμ-*Myc*/*Akt* lymphoma sections stained with haematoxylin and eosin (H/E) or the indicated antibody. **c**, TUNEL (left) and Ki-67 (right) staining (brown) of the indicated lymphoma sections was used to assess apoptosis and proliferation, respectively. **d**, Photomicrographs of haematoxylin-and-eosin-stained liver sections showing perivascular infiltration in control tumours and parenchymal invasion in Akt and Bcl-2 tumours. **e**, **f**, Kaplan–Meier plots showing the tumour-free survival after treatment with CTX (**e**) or DXR (**f**). Mice bearing either control lymphomas (black: DXR, $n = 19$; CTX, $n = 13$), Akt lymphomas (green: DXR, $n = 25$; CTX, $n = 16$) or Bcl-2 lymphomas (blue: DXR, $n = 6$; CTX, $n = 5$) were treated and monitored for time to relapse.

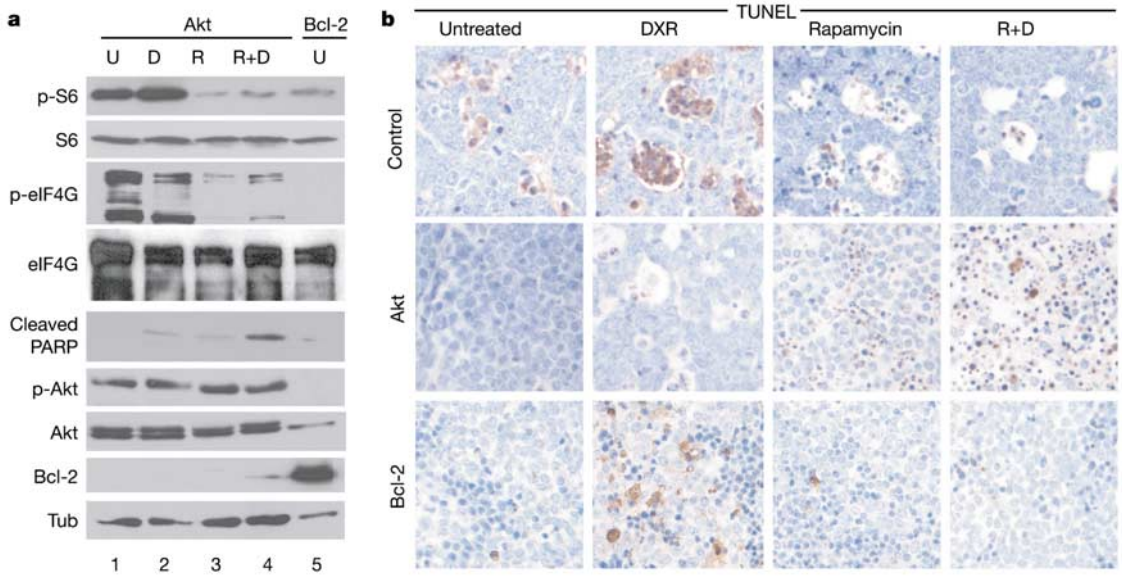

Figure 3 Inhibition of mTOR sensitizes Akt tumours to cytotoxic chemotherapy. Animals harbouring lymphomas of the indicated genotypes were either left untreated (U) or were treated with DXR (D), rapamycin (R) or DXR and rapamycin (R+D), and lymphoma cells were harvested 7 h later. **a**, Lysates were subjected to immunoblotting for phosphorylated and total ribosomal S6 protein (p-S6 and S6), phosphorylated and total eIF4G (p-eIF4G and eIF4G), Akt (p-Akt and Akt), Bcl-2 and α-tubulin (Tub) as a loading control. **b**, Lymphoma sections derived from untreated or treated animals were stained with TUNEL (brown) to identify apoptotic cells.

lymphomas were derived from a more mature B-cell type and often produced an aggressive infiltration of the renal pelvis distinct from Akt-associated pathologies (Fig. 5b; see also Supplementary Fig. 1). Nevertheless, eIF4E is clearly a potent oncogene *in vivo*, producing phenotypes consistent with an anti-apoptotic gene.

Lymphomas expressing eIF4E were highly resistant to DXR therapy relative to controls, and mice harbouring these lymphomas displayed tumour-free and overall survival patterns that were indistinguishable from those harbouring Akt lymphomas (Fig. 5e, $P < 0.0001$ versus control; $P = 0.47$ versus Akt). However, in contrast to Akt lymphomas, eIF4E lymphomas displayed no increase in the rapamycin-sensitive phosphorylation of 4E-BP1 or the S6 ribosomal protein (Fig. 5c), and were non-responsive to rapamycin and DXR therapy *in vivo* (Fig. 5e; see also Fig. 4c, $P < 0.0001$). Furthermore, introduction of eIF4E into an initially sensitive Akt lymphoma conferred resistance to rapamycin and chemotherapy; hence, cells co-expressing eIF4E were enriched in mixed populations after therapy relative to those expressing Akt alone (Fig. 5f, g). Together, these results indicate that eIF4E can recapitulate Akt action in oncogenesis and drug resistance. They also show that eIF4E can confer resistance to a rapamycin-based therapy *in vivo*, presumably because it acts downstream of mTOR.

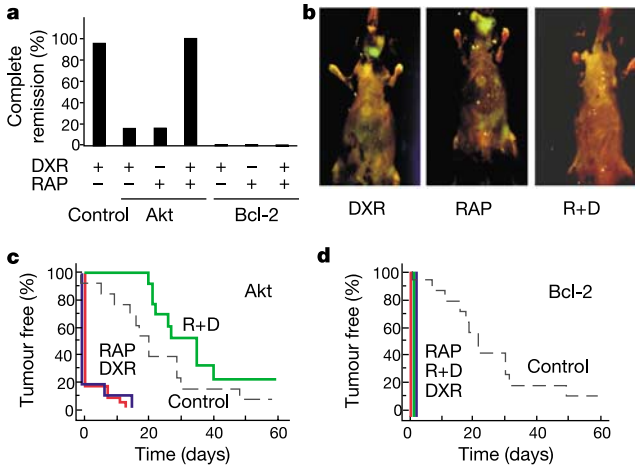

Figure 4 Rapamycin reverses Akt-mediated chemoresistance *in vivo*. **a**, The percentage of mice bearing control ($n = 19$), Akt ($n = 51$) or Bcl-2 ($n = 18$) lymphomas that achieved a complete remission after the indicated treatment. The number of mice in each treatment group ranged from 6 to 25. RAP, rapamycin. **b**, Whole-body fluorescence imaging of GFP expression of a 'matched group' of mice carrying identical Akt tumours 21 days after the indicated treatment. **c**, **d**, Kaplan–Meier plots of tumour-free survival in Akt lymphomas after treatment with DXR (red, $n = 25$), rapamycin (blue line, $n = 12$) and rapamycin plus DXR (green, R+D, $n = 14$) (**c**), and in Bcl-2 lymphomas after treatment with DXR ($n = 6$, red), rapamycin ($n = 6$, blue) and rapamycin plus DXR (R+D, $n = 6$, green) (**d**). The tumour-free survival of the control tumours after DXR treatment is shown for comparison (dotted line).

Our results provide new insights into Akt signalling and tumour behaviour. We find that Akt lymphomas are phenotypically similar to those harbouring a purely anti-apoptotic oncogene with respect to their accelerated onset, aggressive pathology, ability to retain p53 and chemotherapy resistance. Thus, despite its pleiotropic activities, the pro-survival functions of Akt seem sufficient to promote tumorigenesis. Furthermore, we show that the mTOR inhibitor rapamycin can restore apoptotic sensitivity to lymphomas expressing Akt, and that the translation factor eIF4E can recapitulate Akt action *in vivo*. Consequently, a substantial proportion of Akt survival signalling may result from deregulated translation, perhaps through altering the recruitment of pro- and anti-apoptotic mRNAs to polysomes[25,26]. Of note, the apparent role of translational control in cell survival extends to tumours with other PI(3)K pathway lesions, as the chemotherapy resistance of PTEN-deficient lymphomas is reversed by rapamycin in a manner that is also blocked by eIF4E (our own unpublished observations). Together, these results provide *in vivo* evidence that translational signalling through Akt is a broadly relevant oncogenesis and drug-resistance mechanism.

Our results also have important implications for considering the use of targeted therapeutics alone or in combination with conventional agents. By showing that rapamycin can reverse drug resistance in Akt-expressing tumours, we demonstrate that reversing apoptotic defects can restore drug sensitivity *in vivo*. Furthermore, the ability of eIF4E to mediate drug resistance downstream of Akt implies that inhibitors of translation initiation may also be effective

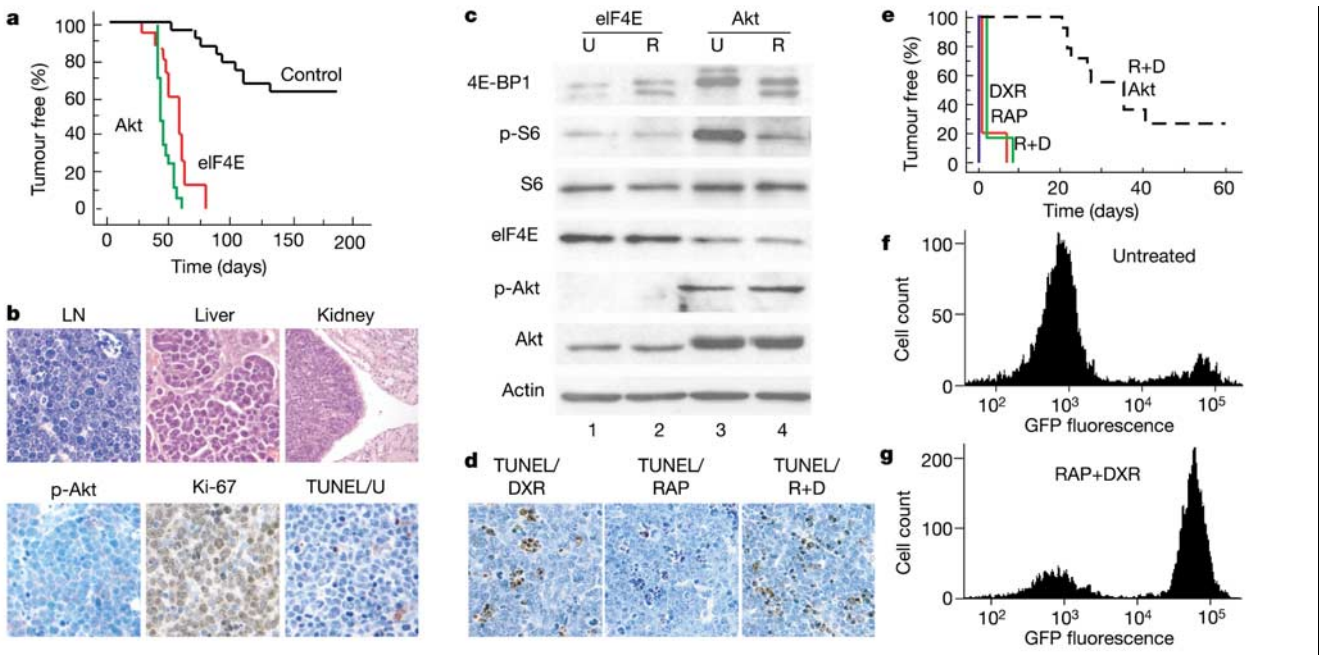

Figure 5 eIF4E promotes oncogenesis and drug resistance *in vivo*. **a**, Kaplan–Meier plots showing tumour onset in mice reconstituted with Eμ-*Myc* HSCs expressing eIF4E (red, $n = 15$). Control and Akt data from Fig. 2 are shown for comparison. eIF4E was unable to induce tumours in normal HSCs within the observation period (>125 days; data not shown). **b**, Representative micrographs of eIF4E lymphoma sections. Top panel, haematoxylin and eosin staining of the indicated organs; lower panel, immunohistochemical stains for phosphorylated Akt, Ki-67 and TUNEL in untreated tumours. LN, lymph node. **c**, Immunoblotting of lysates derived from eIF4E and Akt lymphomas harvested from untreated (U) animals or 6 h after rapamycin (R) administration, using antibodies against the indicated protein ('p' denotes an antibody specific for a phosphorylated protein). Untreated Akt tumours (lane 3) show an increase in the phosphorylated, slower-migrating forms of 4E-BP1. **d**, TUNEL staining (brown) to assess apoptosis in tumour sections harvested 6–8 h after the indicated therapy. **e**, Kaplan–Meier plots showing tumour-free survival of mice bearing eIF4E lymphomas after treatment with DXR ($n = 5$, red line), rapamycin ($n = 6$, blue) and rapamycin plus DXR ($n = 6$, green line). Data from mice bearing Akt lymphomas that had been treated with rapamycin plus DXR are shown for comparison (dotted line). **f**, **g**, *In vivo* competition assay. An Akt lymphoma was transduced with *MSCV–eIF4E–GFP* such that the resulting population contained only about 2–5% GFP-positive cells, and then it was transplanted into multiple recipient mice. Upon lymphoma manifestation, the animals were left untreated (**f**) or treated (**g**) with rapamycin plus DXR therapy. Lymphoma cells were isolated 48 h later and subjected to flow cytometry to determine the fraction of eIF4E-positive cells (high GFP fluorescence).

chemosensitizing agents, and perhaps less prone to resistance. Finally, the selectivity of rapamycin to reverse drug resistance in Akt-expressing lymphomas—despite their broad similarities to those with other apoptotic lesions—implies that the utility of this combination treatment would be missed in clinical trials based solely on tumour type or pathology. Together, our results provide *in vivo* validation for a strategy to reverse drug resistance in human cancers, and underscore the importance of tailoring cancer therapy on the basis of tumour genotype. □

Methods

Generation of lymphomas

Eμ-*Myc* HSCs derived from fetal livers at embryonic day 13–15 were transduced with retroviruses expressing various genes, and used to reconstitute the haematopoietic compartment of lethally irradiated C57BL/6 mice. Eμ-*Myc p53*$^{+/-}$ HSCs were derived from crosses of Eμ-*Myc* and *p53*$^{+/-}$ mice, and detection of loss of heterozygosity in the *p53* locus was by allele-specific PCR[11,27]. The retroviral vectors that were used in this study were *MSCV–GFP* (the empty vector control), *MSCV–Bcl-2*(ref. 12), *MSCV–Akt(myrAkt)*, *MSCV–Akt(K179A)*[9] and *MSCV–eIF4E*. After the appearance of well-palpable lymphomas, tumours were harvested and either fixed for histological evaluation, rendered as single-cell suspensions and frozen in 10% DMSO, or transplanted directly into normal mice for treatment studies[12]. For *in vivo* competition experiments, *MSCV–eIF4E* was transduced into a small percentage of Akt lymphoma cells during a brief *in vitro* passage, and the mixed population was re-injected into several recipient mice. Once lymphomas formed, mice were left untreated or treated with rapamycin and/or DXR. Tumour cells were harvested 48 h later and evaluated for GFP expression by flow cytometry[12].

Treatment studies

A total of 1×10^6 primary lymphoma cells were injected into the tail vein of 6–8-week-old female C57BL/6 mice. After the formation of well-palpable tumours, the animals were treated with rapamycin (4 mg per kg intraperitoneally for 5 days), DXR (10 mg per kg intraperitoneally), CTX (300 mg per kg intraperitoneally) or various combinations. In combination studies, the cytotoxic agent was given on day 2 of the rapamycin protocol. Rapamycin (LC laboratories) was initially dissolved in 100% ethanol, stored at −20 °C, and further diluted in an aqueous solution of 5.2% Tween 80 and 5.2% PEG 400 (final ethanol concentration, 2%) immediately before use. Doxorubicin and cyclophosphamide (both from Sigma) were dissolved in water. In treatment studies, control lymphomas were *Arf*-null tumours arising in an Eμ-*Myc*/*Arf*$^{+/-}$ background[27]. After treatment, the mice were monitored by twice weekly palpation and blood smears.

A complete remission was defined as the absence of detectable tumour and leukaemia. Tumour-free survival was defined as the time between treatment and reappearance of a well-palpable lymphoma[12]. Overall survival was defined as the time between treatment and progression to a terminal stage at which the animals were killed. These data were analysed in the Kaplan–Meier format using the log-rank (Mantel–Cox) test for statistical significance. Whole-body fluorescence imaging of living animals was performed as described[11,28].

Histopathology

Samples were fixed in 10% buffered formalin and embedded in paraffin. Thin sections (5 μm) were stained with haematoxylin and eosin according to standard protocols. Detection of phosphorylated Akt (rabbit antibody against p-Akt Ser 473, 1:100 (Cell Signalling)) and Ki-67 (rabbit antibody, 1:100 (NovoCastra)) was by standard avidin–biotin immunoperoxidase methods, with diaminobenzidine used as the chromogen and haematoxylin as counter stain. For B220 immunohistochemistry (rat antibody against mouse CD45R/B220 clone RA3-6B2 (BD Biosciences, Pharmingen)), antigen retrieval was required. The apoptotic rate was analysed by TUNEL assay according to published protocols[29].

Western blot analysis

Immunoblots were performed from whole-cell lysates[30]. A total of 50 μg of protein/sample were resolved on SDS–PAGE gels and transferred to Immobilon-P membranes (Millipore). Antibodies against phospho-Akt (9275, 1:1,000, Cell Signalling), Akt (9272, 1:1,000, Cell Signalling), ribosomal S6 protein (2212, 1:1,000, Cell Signalling), phospho-ribosomal S6 (2215, 1:1,000, Cell Signalling), cleaved PARP (9548, 1:1,000, Cell Signalling), Bcl-2 (N19, 1:200, Santa Cruz), α-tubulin (B-5-1-2, 1:5,000, Sigma), eIF4E (9742, 1:2,500, Cell Signalling), 4E-BP1 (9452, 1:1,000, Cell Signalling) and β-actin (1:5,000, Sigma) were used as probes and were detected using enhanced chemiluminescence (ECL, Amersham; Lumilight, Roche). eIF4E expression was quantified by immunoblotting using I^{125}-labelled recombinant protein A (PerkinElmer) as a secondary reagent, followed by phosphorimager detection.

Received 13 December 2003; accepted 27 January 2004; doi:10.1038/nature02369.

1. Hanahan, D. & Weinberg, R. A. The hallmarks of cancer. *Cell* **100,** 57–70 (2000).
2. Johnstone, R. W., Ruefli, A. A. & Lowe, S. W. Apoptosis: a link between cancer genetics and chemotherapy. *Cell* **108,** 153–164 (2002).
3. Mayo, L. D., Dixon, J. E., Durden, D. L., Tonks, N. K. & Donner, D. B. PTEN protects p53 from Mdm2 and sensitizes cancer cells to chemotherapy. *J. Biol. Chem.* **277,** 5484–5489 (2002).
4. Datta, S. R., Brunet, A. & Greenberg, M. E. Cellular survival: a play in three Akts. *Genes Dev.* **13,** 2905–2927 (1999).
5. Vivanco, I. & Sawyers, C. L. The phosphatidylinositol 3-kinase AKT pathway in human cancer. *Nature Rev. Cancer* **2,** 489–501 (2002).
6. Steck, P. A. *et al.* Identification of a candidate tumour suppressor gene, MMAC1, at chromosome 10q23.3 that is mutated in multiple advanced cancers. *Nature Genet.* **15,** 356–362 (1997).
7. Sakai, A., Thieblemont, C., Wellmann, A., Jaffe, E. S. & Raffeld, M. PTEN gene alterations in lymphoid neoplasms. *Blood* **92,** 3410–3415 (1998).
8. Min, Y. H. *et al.* Constitutive phosphorylation of Akt/PKB protein in acute myeloid leukemia: its significance as a prognostic variable. *Leukemia* **17,** 995–997 (2003).
9. Andjelkovic, M. *et al.* Role of translocation in the activation and function of protein kinase B. *J. Biol. Chem.* **272,** 31515–31524 (1997).
10. Adams, J. M. *et al.* The c-myc oncogene driven by immunoglobulin enhancers induces lymphoid malignancy in transgenic mice. *Nature* **318,** 533–538 (1985).
11. Schmitt, C. A. *et al.* Dissecting p53 tumor suppressor functions *in vivo*. *Cancer Cell* **1,** 289–298 (2002).
12. Schmitt, C. A., Rosenthal, C. T. & Lowe, S. W. Genetic analysis of chemoresistance in primary murine lymphomas. *Nature Med.* **6,** 1029–1035 (2000).
13. Schmitt, C. A. *et al.* A senescence program controlled by p53 and p16INK4a contributes to the outcome of cancer therapy. *Cell* **109,** 335–346 (2002).
14. Huang, S. & Houghton, P. J. Targeting mTOR signalling for cancer therapy. *Curr. Opin. Pharmacol.* **3,** 371–377 (2003).
15. Plas, D. R., Talapatra, S., Edinger, A. L., Rathmell, J. C. & Thompson, C. B. Akt and Bcl-xL promote growth factor-independent survival through distinct effects on mitochondrial physiology. *J. Biol. Chem.* **276,** 12041–12048 (2001).
16. Edinger, A. L. & Thompson, C. B. Akt maintains cell size and survival by increasing mTOR-dependent nutrient uptake. *Mol. Biol. Cell* **13,** 2276–2288 (2002).
17. Neshat, M. S. *et al.* Enhanced sensitivity of PTEN-deficient tumors to inhibition of FRAP/mTOR. *Proc. Natl Acad. Sci. USA* **98,** 10314–10319 (2001).
18. Grunwald, V. *et al.* Inhibitors of mTOR reverse doxorubicin resistance conferred by PTEN status in prostate cancer cells. *Cancer Res.* **62,** 6141–6145 (2002).
19. Podsypanina, K. *et al.* An inhibitor of mTOR reduces neoplasia and normalizes p70/S6 kinase activity in Pten$^{+/-}$ mice. *Proc. Natl Acad. Sci. USA* **98,** 10320–10325 (2001).
20. Hosoi, H. *et al.* Rapamycin causes poorly reversible inhibition of mTOR and induces p53-independent apoptosis in human rhabdomyosarcoma cells. *Cancer Res.* **59,** 886–894 (1999).
21. Schmelzle, T. & Hall, M. N. TOR, a central controller of cell growth. *Cell* **103,** 253–262 (2000).
22. Lazaris-Karatzas, A., Montine, K. S. & Sonenberg, N. Malignant transformation by a eukaryotic initiation factor subunit that binds to mRNA 5′ cap. *Nature* **345,** 544–547 (1990).
23. Polunovsky, V. A. *et al.* Translational control of the antiapoptotic function of Ras. *J. Biol. Chem.* **275,** 24776–24780 (2000).
24. Hershey, J. W. B. & Miyamoto, S. in *Translational Control of Gene Expression* (eds Sonenberg, N., Hershey, J. W. B. & Mathews, M. B.) 637–654 (Cold Spring Harbor, New York, 2000).
25. Grolleau, A. *et al.* Global and specific translational control by rapamycin in T cells uncovered by microarrays and proteomics. *J. Biol. Chem.* **277,** 22175–22184 (2002).
26. Rajasekhar, V. K. *et al.* Oncogenic Ras and Akt signalling contribute to glioblastoma formation by differential recruitment of existing mRNAs to polysomes. *Mol. Cell* **12,** 889–901 (2003).
27. Schmitt, C. A., McCurrach, M. E., de Stanchina, E., Wallace-Brodeur, R. R. & Lowe, S. W. INK4a/ARF mutations accelerate lymphomagenesis and promote chemoresistance by disabling p53. *Genes Dev.* **13,** 2670–2677 (1999).
28. Yang, M. *et al.* Whole-body optical imaging of green fluorescent protein-expressing tumors and metastases. *Proc. Natl Acad. Sci. USA* **97,** 1206–1211 (2000).
29. Di Cristofano, A., De Acetis, M., Koff, A., Cordon-Cardo, C. & Pandolfi, P. P. Pten and p27KIP1 cooperate in prostate cancer tumor suppression in the mouse. *Nature Genet.* **27,** 222–224 (2001).
30. de Stanchina, E. *et al.* E1A signalling to p53 involves the p19(ARF) tumor suppressor. *Genes Dev.* **12,** 2434–2442 (1998).

Supplementary Information accompanies the paper on **www.nature.com/nature**.

Acknowledgements We thank M. Myers and N. Sonenberg for reagents; C. Rosenthal, M. S. Jiao, P. Chan, M. L. Maunakea and F. Baehner for technical assistance; and L. Bianco for guidance on animal studies. We also thank C. Thompson and members of the Lowe laboratory for discussions, and M. McCurrach, M. Hemann, E. Cepero and D. Burgess for editorial advice. This work was supported by a gift from the Ann L. and Herbert J. Siegel Philanthropic Fund and the Laurie Strauss Leukaemia Foundation, an AACR/Amgen Fellowship in Translational Research (H.-G.W.), a Tularik Post-doctoral Fellowship (E.d.S), a NSERC graduate scholarship (A.M.), an NCI postdoctoral training grant (J.S.F), grants from Canadian Institutes of Health Research and National Cancer Institute of Canada (J.P.), the Mouse Models of Human Cancer Consortium and a Burroughs Wellcome Fund Career Award (S.K.), a SCOR grant from the Leukaemia and Lymphoma Society (S.K and S.W.L.), and a program project grant from the National Cancer Institute (S.W.L and C.C.-C.).

Competing interests statement The authors declare that they have no competing financial interests.

Correspondence and requests for materials should be addressed to S.W.L. (lowe@cshl.edu).

Bmi1 is essential for cerebellar development and is overexpressed in human medulloblastomas

Carly Leung[1]*, Merel Lingbeek[2]*, Olga Shakhova[1], James Liu[1], Ellen Tanger[2], Parvin Saremaslani[1], Maarten van Lohuizen[2] & Silvia Marino[1]

[1]*Institute of Clinical Pathology, Department of Pathology, University of Zürich, Schmelzbergstrasse 12, 8091 Zürich, Switzerland*
[2]*Division of Molecular Genetics, The Netherlands Cancer Institute, Plesmanlaan 121, 1066 CX Amsterdam, The Netherlands*

* These authors contributed equally to this work

Overexpression of the polycomb group gene *Bmi1* promotes cell proliferation and induces leukaemia through repression of *Cdkn2a* (also known as *ink4a/Arf*) tumour suppressors[1,2]. Conversely, loss of Bmi1 leads to haematological defects and severe progressive neurological abnormalities in which de-repression of the *ink4a/Arf* locus is critically implicated[1,3]. Here, we show that Bmi1 is strongly expressed in proliferating cerebellar precursor cells in mice and humans. Using *Bmi1*-null mice we demonstrate a crucial role for Bmi1 in clonal expansion of granule cell precursors both *in vivo* and *in vitro*. Deregulated proliferation of these progenitor cells, by activation of the sonic hedgehog (Shh) pathway, leads to medulloblastoma development[4]. We also demonstrate linked overexpression of BMI1 and patched (PTCH), suggestive of SHH pathway activation, in a substantial fraction of primary human medulloblastomas. Together with the rapid induction of Bmi1 expression on addition of Shh or on overexpression of the Shh target Gli1 in cerebellar granule cell cultures, these findings implicate BMI1 overexpression as an alternative or additive mechanism in the pathogenesis of medulloblastomas, and highlight a role for Bmi1-containing polycomb complexes in proliferation of cerebellar precursor cells.

We characterized the expression of Bmi1 during mouse cerebellar development (at embryonic day (E)14.5 and E16.5 and at postnatal day 1, 5, 8, 15 and 30). Immunohistochemical analysis showed strong nuclear staining for Bmi1 in the cells of the external granular layer (EGL) (Fig. 1, upper row; see also Supplementary Fig. S1) and weaker staining in neural precursor cells of the cerebellar neuroepithelium (Fig. 1, upper row) at all embryonic time points analysed. During postnatal development the strongest Bmi1 staining was observed between days 5 and 8 in actively proliferating granule cell precursors located in the EGL (Fig. 1, middle panel of left column). Immunoblotting of extracts obtained from EGL precursor cells and/or granule cells of newborn mice and mice at postnatal day 5, 8 and 15 confirmed high Bmi1 expression in proliferating granule cell precursors and showed its downregulation in postmitotic and terminally differentiated granule cells (Fig. 1, middle panel of right column). Notably, the time course of this expression paralleled the expression of N-Myc and its target gene cyclin D2 (Fig. 1, middle panel of right column), which are involved in the rapid expansion of progenitor cells during neurogenesis[5–7]. Immunohistochemical staining on autoptic cerebellar sections of human fetuses at gestational week 17, 19, 21, 26 and 32, and of a 2-month-old child and an adult, demonstrate a comparable expression pattern (Fig. 1, bottom panels).

In addition to haematopoietic and skeletal defects, Bmi1-deficient mice develop progressive ataxic gait, balance disorders, tremors and behavioural abnormalities at the age of 2–4 weeks[3]. Although the mice survive to adulthood, they exhibit severe reduction in total postnatal brain mass with particularly severe